Raman scattering from condensed phases of helium. I. Optic phonons in solid helium

R. E. Slusher and C. M. Surko
Bell Laboratories, Murray Hill, New Jersey 07974
(Received 26 August 1975)

Light scattered from solid hcp He crystals contains a sharp spectral feature due to the zone-center optic phonon (ZCOP). We report a study of this ZCOP as a function of molar volume for pure ^{3}He, ^{4}He, and $^4\mathrm{He}_x\,^3\mathrm{He}_{1-x}$ solid mixtures. The dependence on molar volume V of the optic-mode frequency ω_0 for ^{4}He and ^{3}He yields a Grüneisen constant $d\ln(\omega_0)/d\ln(V)$ of 2.6 ± 0.1. The ratio of the optic-mode frequency in ^{3}He to that in ^{4}He at the same molar volume is found to be 1.17 ± 0.01 between 18 and 20 cm^3/mole, confirming the validity of recent theories of short-range correlations in quantum solids. The width $\Delta\omega_0$ of the scattering from the ZCOP was not resolved in any of the pure or mixed crystals, setting a lower limit on the $\omega_0/\Delta\omega_0$ of the mode at 90. Frequencies of the ZCOP in $^4\mathrm{He}_{0.5}\,^3\mathrm{He}_{0.5}$ solids give a Grüneisen constant equal to that in the pure solids. These measurements of phonon frequencies in the mixtures relative to those in the pure solids provide a test of theories of quantum alloys. No local modes were found in the mixed crystals in either bcc or hcp phases.

I. INTRODUCTION

Raman spectra obtained by the scattering of laser radiation from liquids and solids is a powerful and often unique probe of their elementary excitations. This paper reports a more detailed study[1-3] of the scattering of Ar laser light from solid ^{4}He, ^{3}He, and $^4\mathrm{He}_x\,^3\mathrm{He}_{1-x}$ mixtures as a function of molar volume at temperatures near 2 K. A spectrum of the scattered light typical of both pure and mixed hcp He crystals is shown in Fig. 1. The intensity of the scattered light at 90° from the incident laser is plotted as a function of the frequency shift relative to the incident laser frequency. The sharp feature near 9 cm^{-1} is due to Raman scattering from the low-frequency zone-center optic phonon (ZCOP) in hcp helium. The phonon modes of hcp He are shown in Fig. 2 as calculated from self-consistent phonon theory and measured by neutron scattering. The circled point at a wave vector K near zero corresponds to the mode responsible for the sharp peak in Fig. 1. The broad peak and extended tail at high-frequency shifts shown in Fig. 1 is due to multiphonon Raman scattering processes and is discussed in the following paper.[2]

This study of scattering from solid He was motivated by the unique character of helium as a quantum solid. Both ^{3}He and ^{4}He solidify only at pressures greater than 25 atm owing to the weakly attractive interatomic potential and small mass of He atoms. At low pressures ($p \lesssim 100$ atm) the lattice spacing in the solid is larger by (30–40)% than that predicted by the minimum in the interatomic potential. The rms displacement of the He atoms due to quantum-mechanical "zero-point motion" is nearly 30% of the solid lattice spacing. These conditions are related to large anharmonic interactions between neighboring atoms as well as between the phonons. The large displacement of atoms also makes it necessary to account for atoms avoiding each other due to the strong short-range repulsive potential and leads to large short-range correlation effects. Solid helium thus provides a critical test of anharmonic quantum lattice models. It has been shown that for solid helium conventional harmonic models of the lattice vibrations fail completely and a self-consistent phonon

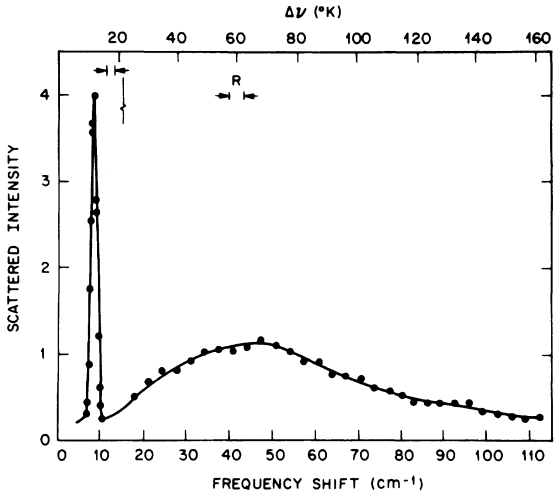

FIG. 1. Typical spectrum of light scattered from solid hcp helium. Intensity at the peak of the sharp feature near 9 cm^{-1} was typically 5–10 counts/sec at the output of the double spectrometer with 50 μ entrance and exit slits. Intensity in the broad peak is normalized to the peak at 9 cm^{-1} but resolution R was decreased to gain signal to noise. These data were taken with a $^4\mathrm{He}_{0.8}\,^3\mathrm{He}_{0.2}$ solid solution at 1.4 K and a pressure of 48 atm.

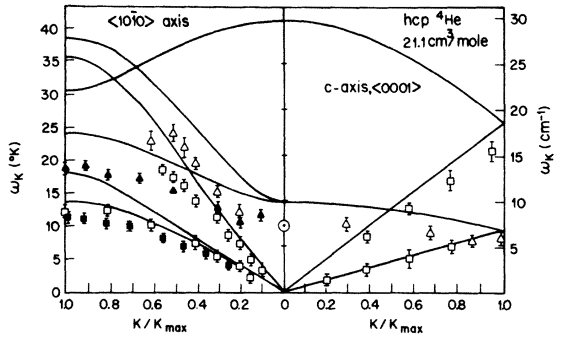

FIG. 2. Phonon dispersion curves for propagation along the c axis, $\langle 0001\rangle$ and $\langle 10\bar{1}0\rangle$ axis in hcp ^{4}He. Solid curves are self-consistent phonon calculations (Ref. 5). Squares and triangles are neutron scattering results for the acoustic and optical branches. The circled point at $K=0$ is extrapolated from the light scattering results in Fig. 4.

(SCP) model including short-range correlations[4,5] is a necessity for description of the lattice modes.

Both neutron[6-8] and light scattering[1] have been used to study the phonon dispersion in solid ^{4}He. Only light scattering data[1] is available for ^{3}He since the large neutron-capture cross section makes neutron scattering in ^{3}He difficult. A typical set of phonon dispersion curves for solid ^{4}He are shown in Fig. 2. Neutron scattering data[6] (squares and triangles) agree qualitatively with the self-consistent phonon calculations[5] (solid lines). However at 21.1 cm^3/mole the high-frequency optic mode is not observed, probably because of its large widths. For propagation along the c axis the optic modes correspond to a high-frequency LO branch for opposed motion of the two atoms in the hcp unit cell and a low-frequency TO branch (triangles in Fig. 2) for opposed motion transverse to the c axis. The high-frequency optic mode is not Raman active because of the symmetry of the mode. The Raman-active low-frequency optic mode is responsible for the sharp line in Fig. 1 and corresponds to the circled point at the zone center in Fig. 2.

For solid He the light scattering can be described in terms of the interaction of the electric dipoles induced at each He atom by the incident laser field.[9] At each atomic site $\vec{r}_i$ the effective electric field can be approximated by the sum of incident field and the induced dipole fields of neighboring atoms at positions $\vec{r}_j$,

$$\vec{E}(\vec{r}_i,t)=\vec{E}_0(\vec{r}_i,t)+\sum_j \vec{E}_{dij}\ , \tag{1}$$

where the incident laser field is

$$\vec{E}_0=\vec{E}_{00}\,e^{i(\omega_L t-\vec{k}_L\cdot\vec{r}_i)}\ ,$$

and the induced dipole field in first order is

$$\vec{E}_{dij}=\alpha_0\left(\frac{\vec{E}_0\cdot\hat{r}_{ij})\hat{r}_{ij}}{|\vec{r}_{ij}|^3}-\frac{\vec{E}_0}{|\vec{r}_{ij}|^3}\right); \tag{2}$$

ω_L and $\vec{k}_L$ are the incident laser frequency and wave vector and $\vec{r}_{ij}$ is $\vec{r}_i-\vec{r}_j$. The relative atomic positions oscillate at the lattice mode frequencies ω_0. The induced polarization for an atomic polarizability α_0 is

$$\vec{P}(\vec{r}_i,t)=\alpha_0\vec{E}(\vec{r}_i,t)\ , \tag{3}$$

$$\vec{P}(\vec{r}_i,t)=\alpha_0\left[\vec{E}_0+\alpha_0\sum_j\left(\frac{3(\vec{E}_0\cdot\hat{r}_{ij})\hat{r}_{ij}}{|\vec{r}_{ij}|^3}-\frac{\vec{E}_0}{|\vec{r}_{ij}|^3}\right)\right]. \tag{4}$$

The dipolar field terms in Eq. (4) cause frequency mixing between the oscillatory terms in $\vec{E}_0$ and $\vec{r}_{ij}$ which results in scattered radiation at frequencies

$$\omega=\omega_L-\omega_0\ . \tag{5}$$

A Raman scattering efficiency follows from the square of the polarization given in Eq. (4) and is given by (see Ref. 9 for an accurate detailed derivation)

$$\mathcal{R}\simeq 6.5\,\frac{nN}{V}\left(\frac{\omega_L}{c}\right)^4\left(\frac{u}{a}\right)^2\frac{\alpha_0^4}{a^6}\,\epsilon_{1\perp}^2\,\epsilon_{2\perp}^2$$

$$\approx 3\times10^{-11}\ \mathrm{cm^{-1}\,sr^{-1}}\ , \tag{6}$$

where u is the zero-point motion amplitude $(\pi\hbar/M\omega_0)^{1/2}$ about the equilibrium atomic positions at spacings a, and $\epsilon_{1\perp}$ and $\epsilon_{2\perp}$ are the components of the incident and scattered light polarizations perpendicular to the c axis of the hcp crystal. The small value of α_0 for helium compared with the other rare gases results in a weak scattering efficiency, however, the $(u/a)^2$ factor enhances the efficiency because of the large zero-point motion in helium.

The experimental apparatus for measuring the relatively weak scattering is described in Sec. II. In Sec. III we discuss the optic phonon widths and frequencies as a function of molar volume for isotopically pure crystals. In Sec. IV the behavior of the optic phonon in $^4\mathrm{He}_x{}^3\mathrm{He}_{1-x}$ solid solution is presented and discussed in terms of recent calculations of the force constant renormalization for quantum alloys.

II. EXPERIMENTAL APPARATUS

The experimental apparatus is shown in Fig. 3. Helium samples were prepared in a 3.3-cm^3 copper-berylium cell (C in Fig. 3) mounted on top of a pumped liquid-^{4}He pot. The top of the cell could be heated to grow, anneal, or melt helium crystals. Germanium thermometers monitored the

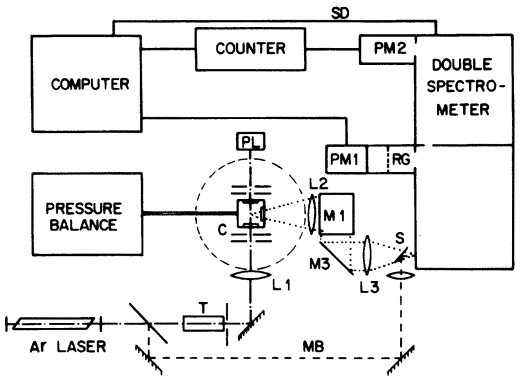

FIG. 3. Schematic diagram of apparatus for light scattering from solid helium. Solid helium is grown in Cu:Be cell C mounted on 1-K pot in the Dewar shown as dashed circle. Incident Ar laser is focussed into cell through telescope T and lens $L1$ and its power is monitored at PL. Scattered light is collected with lens $L2$, its image is rotated by mirrors $M1$–$M3$ and focused into the double spectrometer with lens $L3$. Scattered light is detected with a channeltron PM2, and then counted and stored in the computer. The spectral position of the scattered light is monitored by the weak split out beam MB which passes through the first section of the spectrometer and Ronchi grating RG and is detected at PM1. The computer stores the Ronchi monitor signal and controls the spectrometer drive as indicated by SD.

temperature at the top and bottom of the cell. The Cu:Be heat conductivity was sufficient to maintain the temperature of the He sample constant to within ±0.1 K with the heater off. Helium entered the cell through a small capillary tube after being filtered by a crushed stainless plug at 4.2 K. Dust or ice particles which cause heating and elastic light scattering in the focal volume of the incident laser are trapped by this filter. The capillary tubing could be heated to prevent blocking with solid He. Pressurized helium in the cell was obtained either from gas supply bottles or by an oil or mercury pressure balance. Helium crystals were grown over a period of 30 min to 1 h at constant pressure to obtain good optical quality (i.e., no bubbles, grain boundaries, etc.). These crystals were observed to be transparent except for a few small scattering centers probably due to residual dust and ice particles. The Brillouin scattering in the focal volume of the incident laser is visible as a faint green line in the crystal. Mixed $^4He_x{}^3He_{1-x}$ crystals required slower growth and longer annealing periods in order to obtain good optical quality and uniform composition of the mixture. The ratio of ^3He to ^4He was monitored by two techniques, both indicating that there was no separation of ^3He from ^4He. First the gas in the room-temperature portion of the capillary feeding the cell was analyzed during and after the experiment and no ^3He enrichment over the initial concentration was found. Second, the pressure and temperature of the hcp-to-bcc transition was monitored by the disappearance of the sharp optic-mode Raman scattering and was found to occur at the previously reported point of the phase diagram.[10] The pressure was kept nearly constant and the capillary was heated to prevent blockage as the crystal grew; however, since the heaters were turned off after the crystal was grown, the actual pressure in the cell was uncertain within ±3%. Optical access to the sample was provided with three $\frac{1}{8}$-in.-thick 0°-oriented sapphire windows each sealed with a pair of indium-alloy O rings. These sapphire windows do not crack (as quartz did) above 100 atm, however they do cause a depolarization of the incident and scattered light by (20–30)% making it difficult to obtain results on the relative polarization of the scattering.

Raman spectra were excited with an Ar laser beam at 5145 Å. The power was varied between 0.1 and 1 W depending on the temperature control desired. A uniform heating in the He sample of a $\frac{1}{10}$ deg/W of incident light was caused by light scattering from optical imperfections. Scattered light was kept at a minimum by apertures in the dewar. Light scattered at 90° was collected with an $f/3$ lens ($L2$), passed through a system of three mirrors to form a vertical image, then focused into the spectrometer with an $f/7$ lens ($L3$). The weak scattered light (~1–50 counts/sec) was spectrally analyzed with a double grating spectrometer and detected with a channeltron photomultiplier (PM2). The leaked light and dark count rate of the system totaled ~0.1 counts/sec with 50-μ entrance and exit slits and a 150-μ center slit. Data was averaged over multiple sweeps of the spectrometer using the computer which also controlled the spectrometer drive.

The frequency shifts and widths for the Raman spectra of solid He required an absolute precision of ±0.1 cm^{-1}. The Spex 1400 double spectrometer used in these experiments had a wavelength monitor dial which was geared to the grating drive and gave the spectral position to no better than ±0.5 cm^{-1}. This uncertainty was caused in part by thermal drifts and mechanical linkages. The required precision was obtained[11] by splitting out 3% of the incident laser beam to monitor the grating position (see Fig. 3). The monitor beam was focused with an $f/20$ lens into the upper portion of the entrance slit of the spectrometer which was not illuminated with scattered light from the cell. After reflection from the first grating the monitor beam was intercepted by a mirror at the center slit of the double spectrometer and focused on a Ronchi ruling. The spacing of the transparent re-

gions of the Ronchi grating was chosen nearly equal to the entrance slit width. A photomultiplier monitored the intensity behind the Ronchi ruling which varied periodically as the grating swept. These periodic variations were calibrated by the rotational line of molecular nitrogen gas. This system provided a constant monitor of the spectral pass region to within ± 0.05 cm^{-1}. The Ronchi monitor signal was stored in the computer and any irregular or drifted spectral scans were automatically rejected.

III. RESULTS FOR PURE SOLID

A. Optic phonon frequencies in pure He solids

The Raman spectra of hcp helium has two prominent features as shown in Fig. 1. These data are a result of averaging 50 sweeps of the spectra with a dwell time at each point of 1 sec. The sharp line at a frequency shift of 8.5 cm^{-1} is due to the creation of a single zone-center Raman-active optic phonon (the point circled in Fig. 2). The broad peak near 45 cm^{-1} is due to multiphonon Raman scattering and is discussed in detail in the following paper.

The frequency shift of the sharp single phonon line is shown in Fig. 4 as a function of molar volume for pure ^{4}He, pure ^{3}He, and a ^{4}He$_{0.5}$^{3}He$_{0.5}$ mixture. The ZCOP frequencies shift nearly linearly with molar volume, and the light scattering data are in good agreement with the zone-center frequency obtained from fits to the neutron scattering data (squares in Fig. 4). The major error in the light scattering data is due to an uncertainty of ± 0.1 cm^3 in the molar volume caused by remote monitoring of the cell pressure.

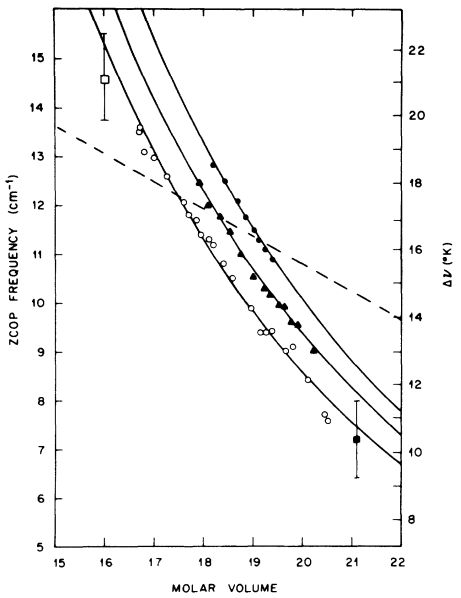

FIG. 4. Molar volume dependence of the frequency of the zone-center optic phonon in pure hcp ^{4}He (open circles), pure hcp ^{3}He (solid circles), and a ^{4}He$_{0.5}$^{3}He$_{0.5}$ hcp solution (solid triangles). The open square is a neutron scattering point from Ref. 7 and the solid square from Ref. 6. Solid curves are least-squares fits to the data assuming a volume-independent Grüneisen parameter. The dashed curve is a computer calculation from the self-consistent phonon theory (Ref. 5).

The neutron scattering experiments[7,8] show that for all branches phonon frequencies throughout the zone scale uniformly to within $\pm 10\%$ with molar volume. This implies the ZCOP shift is proportional to the Debye temperature and can be related to the Grüneisen parameter

$$\gamma(V) = -\frac{V}{\omega_0}\frac{d\omega_0}{dV} = -\frac{d\ln(\omega_0)}{d\ln(V)}, \tag{7}$$

where ω_0 is the ZCOP frequency and V is the molar volume. The Grüneisen parameter is a measure of the anharmonicity of the lattice and characterizes a solid through the Mie-Grüneisen equation of state[12,13]

$$P(T, V) = P_0(V) + \gamma(V)U/V, \tag{8}$$

where $P(T, V)$ is the pressure of the solid as a function of volume and temperature and U is the temperature-dependent internal energy of the crystal. In first order γ is a constant independent of volume. In this approximation the solid lines in Fig. 4 are least-squares fits to Eq. (7) yielding Grüneisen constants of 2.6 ± 0.1 for both ^{4}He and ^{3}He. Specific-heat[14] and[15] $(\partial P/\partial T)_V$ data have been used to obtain similar values of γ through Eq. (8). Ahlers[14] specific-heat measurements were over a sufficient range to determine a volume dependence of γ as an expansion of the form

$$\gamma(V) = c_1 + c_2 V, \tag{9}$$

where $c_1 = 1.02$ and $c_2 = 0.083$ were the constants for hcp ^{4}He determined by fits to experimental data. Although the data in Fig. 4 are not accurate enough over an extended range of molar volumes to determine c_1 and c_2 independently, if c_1 is fixed at 1.02, a c_2 of 0.083 ± 0.03 is found from a least-square fit to the ^{4}He data in Fig. 4. An analysis of Ahler's ^{4}He data[14] and ^{3}He specific-heat data by Sample and Swenson[16] shows that the ratio of γ in ^{3}He to that in ^{4}He is unity in good agreement with the results obtained from the data shown in Fig. 4.

The ratio of the ^{3}He to ^{4}He ZCOP frequency at the same molar volume is an interesting test of the effective force constants and short-range correlation in solid He. For harmonic solids with the same atomic spacings (i.e., same molar volumes) the frequency ratio ω_{03}/ω_{04} of ^{3}He relative to ^{4}He

should be the square root of the mass ratio 1.155. The ratios found from the fitted functions [Eq. (7) and solid lines in Fig. 4] range between 1.17 and 1.18. These values are consistent with the ratio of Debye temperatures in hcp ^{3}He and ^{4}He, of 1.17–1.2 found in Ahlers[14] analysis. Greywall[17] has obtained isotope ratios of 1.2–1.25 for transverse acoustic-phonon frequencies and 1.3–1.36 for longitudinal acoustic phonons in bcc helium at 21 cm^3/mole from sound velocity measurements.

All of these experimental ω_{03}/ω_{04} ratios are higher than the ratio predicted for simple harmonic solids if the force constant is the same for both isotopes. At first one might hope to explain these isotope results by the larger zero-point motion of ^{3}He causing an atom to experience larger values of the second derivative of the effective potential at short range. This would cause an effective increase in the force constants for ^{3}He relative to ^{4}He in agreement with the experimental trend. But this argument neglects the effects of short-range correlations (i.e., the tendency of helium atoms to avoid each other because of strong repulsive interactions). Nosanow[18] used an empirical Jastrow function of the form

$$f(r) = e^{-KV(r)/4E}, \tag{10}$$

where K is a constant, $V(r)$ is the pair potential and E is the energy minimum of $V(r)$. A self-consistent phonon calculation[5] using this Nosanow-Jastrow function with the same K for both ^{3}He and ^{4}He gives an isotope frequency ratio for the ZCOP of only 1.08, much less than the observed ratios of 1.17–1.18. These calculations yield a volume dependence for the ZCOP shown by the dashed line in Fig. 4, obviously in disagreement with neutron and light scattering data. Improved agreement between these calculations[5,22] and the data can be obtained by varying the constant in the exponent of the Nosanow-Jastrow function. Werthamer[19] has shown that the functional form of the Jastrow function can be optimized by a self-consistent Schrödinger equation solution. Other approaches to the theory of short-range correlations are the T-matrix theory used by Glyde and Khana[20] and a similar matrix theory used by Horner.[21] The Jastrow functions obtained from these theories do not attenuate the strong repulsive potential as sharply as the Nosanow-Jastrow function. This weaker cutoff is seen in Fig. 3 of Ref. 19, and should tend to increase the ω_{03}/ω_{04} ratios because of increased penetration of the ^{3}He wave function into the region of strong repulsion. This tendency is found in the numerical calculations provided by Glyde[22] and shown in Table I. It is clear that for these zone-boundary phonons in bcc helium the T-matrix theory gives higher isotope ratios than the Nosanow-Jastrow function. It can also be seen that when K is allowed to vary so as to minimize the ground-state energy (middle column in Table I; $K = 0.17 \pm 0.005$ for ^{3}He and $K = 0.21 \pm 0.005$ for ^{4}He) the isotope ratio is higher than when it is kept the same for both ^{3}He and ^{4}He (last column in Table I, $K = 0.17$ for ^{3}He and ^{4}He). It is not clear why the variationally determined cutoff is stronger in ^{4}He than in ^{3}He. The isotope ratios are further modified when the cubic anharmonic term and higher-order anharmonic terms[23] are added. Although the calculations have not been done for hcp helium, the ratios obtained from the

TABLE I. Isotope frequency ratios computed by Glyde for phonon frequencies in bcc ^{3}He and ^{4}He, both at $V = 19.00$ cm^3/mole. Q is the phonon wave vector and L and T refer to the longitudinal and transverse modes.

Q	ω_3/ω_4								
Units of $2\pi/a$	Glyde-Khanna T matrix			Nosanow-Jastrow			Identical Nosanow-Jastrow		
	L	T_1	T_2	L	T_1	T_2	L	T_1	T_2
[100]									
1	1.162	1.162		1.099	1.099		0.982	0.982	
0.7	1.177	1.158		1.141	1.091		1.038	0.971	
0.5	1.195	1.152		1.174	1.080		1.081	0.953	
0.05	1.221	1.143		1.205	1.057		1.107	0.920	
[110]									
0.5	1.187	1.208	1.144	1.159	1.143	1.050	1.067	1.082	0.912
0.05	1.190	1.196	1.143	1.163	1.139	1.057	1.042	1.095	0.920
[111]									
0.5	1.183	1.183		1.143	1.143		1.055	1.055	
0.05	1.184	1.162		1.153	1.095		1.027	0.990	

T-matrix theory are much closer to the experimental ratios than a similar calculation using the Nosanow-Jastrow function. The T-matrix theory[19] also gives a Grüneisen constant (defined in terms of the acoustic velocity) of 2.0–2.6 for 24-cm^3/mole bcc ^{3}He while the Nosanow-Jastrow function gives 1.5–1.8. These theoretical values should be compared to an experimental value of 2.2,[19] again indicating that the Nosanow-Jastrow function cuts off the effective potential too rapidly. Horner's[21] calculations are also in good agreement with both the experimental isotope ratios[17] and the molar volume dependences of the phonon frequencies for bcc He.

B. Scattered intensities

For an incident laser power of 0.5 W the scattered light counting rate at the output of the double spectrometer (see Fig. 3) was typically 5–15 counts/sec at the peak of the ZCOP mode with 75-μ entrance and exit spectrometer slits. The 75-μ slit width matched the width of the optical image of the focal volume and corresponded to a 1.7-cm^{-1} full width at half-maximum (FWHM) (including laser linewidth of 0.2 cm^{-1}). The relative intensity of the sharp ZCOP mode to the broad peak at higher frequency shifts is shown in Fig. 1 for a fixed spectrometer slit width of 50 μ.

For an absolute measure of the Raman scattering efficiency from the ZCOP a comparison can be made with the Brillouin scattering efficiency.[24] Brillouin scattering is unresolved around the laser frequency in these experiments and was the major contribution to the "elastically" scattered light for liquid and very clean solid helium. The Brillouin scattering decreases by a factor of 3–10 when helium, initially at vapor pressure, is pressurized to form a solid. Scattering from imperfections in solid crystals was often of the same order of magnitude as the Brillouin scattering so that a better comparison of the phonon scattering is made by comparison with the roton scattering (which has been related to the Brillouin scattering[24]). Scattering at the peak of the roton feature ($T = 1.3$ K) was 1.3 times the phonon scattering with identical optical alignment and 75-μ spectrometer slit widths. A Raman efficiency $\mathcal{R}$ of $(5 \pm 3) \times 10^{-13}$ cm^{-1} sr^{-1} for the ZCOP is thus obtained. Using a mean value of the incident and scattered polarizations, nN/V of 3×10^{22} cm^3, α_0 of 2×10^{-25} cm^3, ω_0/c of 1.2×10^5 cm^{-1}, M of 6.6×10^{-24} g, and u/a of 0.2, a Raman efficiency $\mathcal{R}$ of 7×10^{-13} cm^{-1} sr^{-1} is obtained from Eq. (6) in good agreement with measured value.

Variations of no more than (20–50)% in intensity were noted between helium crystals of ^{3}He, ^{4}He, or $^4\mathrm{He}_x{}^3\mathrm{He}_{1-x}$ mixed crystals and these variations could have resulted from variations in optical alignment. The Raman efficiency is expected to vary as V^{-3} or a factor of 1.9 over the range of ^{4}He molar volumes investigated. However, the incident and scattered polarization were not well enough defined (because of the sapphire windows) to check this dependence.[25]

C. Optic-phonon width

A study of the width of the scattering from the ZCOP was made using the Ronchi grating frequency monitor described in Sec. II. With 50-μ entrance and exit slits the observed linewidth for single phonon scattering is 1.2 ± 0.05 cm^{-1} (FWHM). This width is fully accounted for by the spectrometer resolution (1 cm^{-1}) and the 0.2-cm^{-1} width of the laser oscillating over a range of longitudinal modes. A scan of the elastically scattered laser light has a spectral profile identical to the scattering from the optic phonon. This sets a lower limit on the Q of the phonon (defined as its frequency divided by the FWHM width) at 90.

It is expected that the major contribtuion to the width of the ZCOP in a pure crystal is the decay to two acoustic phonons due to the large third-order anharmonic terms in the potential. Calculations of the width due to these terms by scp methods give estimates[26] of Q in the range from 10^3–10^4, well within the limits set by the present data. The two-phonon decay process is enhanced by the anharmonicity resulting from the large zero-point motion in solid He, however, energy and momentum conservation require the wave vectors of the acoustic-phonon decay products to be in the range of $\frac{1}{3}$ the zone-boundary wave vector. This mismatch between the acoustic-phonon wavelength and the atomic spacing (characteristic of the optic-phonon normal mode) reduces the strong anharmonic decay and results in the large Q for the zone-center optic branch.

IV. SOLID SOLUTIONS OF ^{3}He and ^{4}He

A. Optic-phonon frequencies and widths

Solid solutions of ^{3}He and ^{4}He in the hcp phase were found to have scattering spectra nearly identical to the pure solids except for a shift in frequency of the sharp ZCOP feature. As shown in Fig. 1 for a $^4\mathrm{He}_{0.8}{}^3\mathrm{He}_{0.2}$ spectra, the sharp ZCOP and broad peak at higher frequency shifts were identical in form and relative intensity to the spectra of the pure solids. The optical quality of solid solutions was poorer than for pure solids and longer annealing times were required to produce "clear" crystals.

The most accurate data for the frequency of the ZCOP feature as a function of molar volume was

taken with a $^4He_{0.5}{}^3He_{0.5}$ crystal as shown in Fig. 4. As in the pure solid the data can be fit to a volume-independent Grüneisen constant. The best fit of $\gamma = 2.56 \pm 0.1$ is the same within experimental error as for both pure solids. Using this fit to the experimental data the ratio of the ZCOP frequency in the $^4He_{0.5}{}^3He_{0.5}$ solution, ω_{034}, to the frequency in ^4He is $\omega_{034}/\omega_{04} = 1.09 \pm .01$. As in the pure solids the width of the ZCOP scattering feature was not resolved in the solutions giving a lower limit on Q of greater than 90 for this mode.

B. Local modes

No evidence for local modes is seen in the spectra of the $^4He_{0.8}{}^3He_{0.2}$ as shown in Fig. 1 and none were found at other pressures and concentrations. Local modes, e.g., corresponding to a ^3He atom vibrating in a cluster of ^4He atoms should result in a sharp peak on the broad high-frequency shift spectra in Fig. 1. A null search was also made for local modes in the bcc phase of $^4He_{0.8}{}^3He_{0.2}$ solid. This absence of local modes is not surprising since the mass defect for ^3He in ^4He,

$$\epsilon = (m_4 - m_3)/m_4 = 0.25 , \tag{11}$$

is small. A theoretical model[27] of solid Ar predicts no local modes in the cubic phase for ϵ less 0.3. The saddle point in the dispersion relation for solid hcp helium near the zone center may increase the minimum value of ϵ for a local mode in $^4He_x{}^3He_{x-1}$ solutions. If there were a local mode in the bcc phase of the solutions its frequency would be split off from the zone-boundary phonon frequency ω_b by a frequency of the order of $\epsilon^2\omega_b \sim 1\ \mathrm{cm}^{-1}$.[28] This value is small compared to the width[6-8] of the zone-boundary modes in solid He, and interaction of the zone boundary and local modes should produce appreciable broadening of the local mode.

C. Linear-chain model for $^4He_{0.5}$ $^3He_{0.5}$ solution

A simple model of the excitation in a alloy has recently been used to estimate the frequencies of magnetic excitations in a two-dimensional random antiferromagnet.[29] This model can be used to estimate the vibrational frequencies in a random linear-chain with two inequivalent sites. This is a much simplified model of a $^4He_x{}^3He_{1-x}$ solution where there are two inequivalent sites in the hcp unit cell and modes near $k = 0$ may not be highly dependent of crystal structure. For He the lattice constants for the solutions can be adjusted experimentally and one can compare the pure crystals and solutions at constant molar volume, i.e., atomic spacing. It is also assumed in first order that the force constants are the same for both pure crystals and solutions.

Consider the chain of atoms coupled by two different force constants c_1 and c_2 whose sites are occupied randomly by ^3He or ^4He:

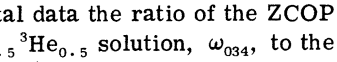

The equations of motion for the site $2i$ are

$$-(M_4, M_3)\,\ddot{U}_{2i} = c_1(U_{2i} - U_{2i+1}) + c_2(U_{2i} - U_{2i-1}) , \tag{12}$$

where U_{2i} is the displacement of the atom at site $2i$. The occupation of the site is described by x_{2i} which is $+1$ for ^4He occupancy and -1 for ^3He occupancy, so that

$$\tfrac{1}{2}(1 + x_{2i})\,U_{2i} = {}^4U_{2i} \tag{13}$$

and

$$\tfrac{1}{2}(1 - x_{2i})\,U_{2i} = {}^3U_{2i} . \tag{14}$$

One then obtains four coupled equations of the form

$$-M_4^4\ddot{U}_{2i} = c_1[{}^4U_{2i} - \tfrac{1}{2}(1 + x_{2i})({}^4U_{2i-1} + {}^3U_{2i-1})] + c_2[{}^4U_{2i} - \tfrac{1}{2}(1 + x_{2i})({}^4U_{2i+1} + {}^3U_{2i+1})] . \tag{15}$$

In order to estimate the mean spectral position of the phonon modes these equations are now averaged and for a $^4He_{0.5}{}^3He_{0.5}$ solution in first-order the terms linear in x are dropped since x is randomly $+1$ and -1 along the chain. This averaging procedure is motivated by its success in predicting the dispersion relations of magnetic excitations in magnetic alloys.[29] After Fourier transforming the set of four averaged equations one obtains

$$\omega^2 M_j^j U_e = (c_1 + c_2)^j U_e - (c_1 e^{ika} + c_2 e^{-ika})[\tfrac{1}{2}({}^4U_0 + {}^3U_0)], \tag{16}$$

$$\omega^2 M_j^j U_0 = (c_1 + c_2)^j U_0 - (c_1 e^{-ika} + c_2 e^{ika})[\tfrac{1}{2}({}^4U_e + {}^3U_e)], \tag{17}$$

where U_0 and U_e are the Fourier amplitudes of the mode at wave vector k at odd and even sites, respectively, and j indicates the occupancy of the site by ^3He or ^4He. These equations are easily solved at $k = 0$, the case of interest for the ZCOP in solid helium. The normal-mode frequencies are

$$\omega^2 = 2(c_1 + c_2)/m_{\mathrm{eff}} . \tag{18}$$

The effective mass, m_{eff} is given by

$$1/m_{\text{eff}} = (1/2\sqrt{M_4 M_3})\tfrac{1}{2}(1/\rho + \rho)(1 \pm \tfrac{1}{2}) \pm \{[\tfrac{1}{2}(\rho + 1/\rho)]^2(1 \pm \tfrac{1}{2})^2 - (1 \pm 1)\}^{1/2}, \quad (19)$$

where

$$\rho = \sqrt{M_4/M_3}\,. \quad (20)$$

This model is valid only for $c_1 \simeq c_2$ and for $^3He_{0.5}$ $^4He_{0.5}$. The four solutions for the frequency ratio of interest are

$$\omega_{034}/\omega_{04} = 1.091, 0.764, 0.749, 0. \quad (21)$$

The first solution is in good agreement with the measured value of 1.09 ± 01. In this linear-chain model ω_{03}/ω_{04} is the harmonic ratio 1.155. No evidence for the nearly degenerate modes at ω_{034}/ω_{04} of 0.764 and 0.749 was found. Although this model is too simple to obtain any quantitative predictions of the ω_{034}/ω_{04} ratio, the measured ratio is close to the predicted value of 1.091 using this harmonic theory with the same force constants for pure and mixed crystals.

We conclude that there are no adequate theories for the phonons at present which include both the effects of random occupation of the lattice sites and changes in the effective force constants. Predictions of the force-constant changes for isolated isotopic impurities in solid helium have been made by Varma[30] and Nelson and Hartmann,[31] but these predictions do not apply for the results presented here because of the nearly equal isotopic concentrations.

V. CONCLUSIONS

The molar volume dependence of the ZCOP frequency in hcp helium as determined by Raman scattering is similar for both the pure solids and ^4He_x $^3He_{1-x}$ solid solutions. A volume-independent Grüneisen constant of 2.6 ± 0.1 characterizes all helium solids for temperatures between 1 and 2 K and molar volumes from 17 to 21 cm^3/mole. At constant molar volume the frequency ratios between the pure solid ^{4}He and ^{3}He provide an important test of short-range correlation effects in quantum solids. The measured ratio ω_{03}/ω_{04} for the ZCOP of 1.17–1.18 are larger than the square root of the mass ratio 1.155. These measured ratios tend to agree with the T-matrix theories[20,22] of short-range correlation much better than the empirical Nosanow-Jastrow function.[5,18] Comparison of these experimental results for ω_{03}/ω_{04} and more detailed calculations for the hcp structure should provide good quantitative tests of these short-range correlation theories. These results should compliment similar studies of the molar volume dependence of acoustic-phonon frequencies.

All solids studied here had ZCOPs with a Q of greater than 90. This is in agreement with theory for the pure solids but is not explained for the ^4He_x $^3He_{1-x}$ solutions. The absence of local modes in the solid solutions found in these experiments is not surprising because of the small mass defect for helium isotopes. In general, helium is an interesting system for study of solutions since the lattice spacing can be easily varied. There still remain several unanswered questions concerning phonon linewidths, force constants, and short-range correlations.

ACKNOWLEDGMENTS

We would like to thank H. R. Glyde, W. M. Hartmann, L. R. Walker, N. R. Werthamer, and C. M. Varma for helpful discussions and assistance with theoretical calculations. We thank H. R. Glyde for computing the ω_3/ω_4 ratios for T-matrix and Nosanow-Jastrow theories. We thank D. S. Greywall for comminicating his results on acoustic-phonon frequency ratios prior to publication. We thank M. Rhinewine for technical assistance.

[1] R. E. Slusher and C. M. Surko, Phys. Rev. Lett. 27, 1699 (1971).

[2] C. M. Surko and R. E. Slusher, following paper, Phys. Rev. B 13, 1095 (1976).

[3] C. M. Surko and R. E. Slusher, in *Low Temperature Physics-LT 13*, edited by K. D. Timmerhaus, W. J. O'Sullivan, and E. F. Hammel (Plenum, New York, 1974), Vol. 2, pp. 100–104.

[4] Several reviews of lattice vibrations in solid He are now available, e.g., C. M. Varma and N. R. Werthamer, in *The Physics of Liquid and Solid Helium*, edited by K. Benneman and J. Ketterson (Wiley, New York, 1976).

[5] N. S. Gillis, T. R. Koehler, and N. R. Werthamer, Phys. Rev. 175, 1110 (1968).

[6] V. J. Minkiewicz, T. A. Kitchens, F. P. Lipschultz, R. Nathans, and G. Shirane, Phys. Rev. 174, 267 (1968).

[7] T. O. Brun, S. K. Sinha, C. A. Swenson, and C. R. Tilford, in *Neutron Inelastic Scattering* (IAEA, Vienna, 1968); R. A. Reese, S. K. Sinha, T. O. Brun, and C. R. Tilford, Phys. Rev. A 3, 1688 (1971).

[8] V. J. Minkiewicz, T. A. Kitchens, G. Shirane, and E. G. Osgood, Phys. Rev. (to be published).

[9] N. R. Werthamer, Phys. Rev. 185, 348 (1969); N. R. Werthamer, R. L. Gray, and T. R. Koehler, Phys. Rev. B 4, 1324 (1971).

[10] C. le Pair, K. W. Taconis, R. de Bruyn Ouboter, E. de Jong, and J. Pit, in *Low Temperature Physics*

LT 9, edited by J. G. Daunt, D. O. Edwards, F. J. Milford, and M. Yagub (Plenum, New York, 1965), part A, pp. 234–239.
[11]M. Rhinewine, Rev. Sci. Instrum. 46, 448 (1975).
[12]For an introduction to the Grüneisen constant see C. Kittel, *Introduction to Solid State Physics* (Wiley, New York, 1967), 3rd ed., p. 182.
[13]C. A. Swenson, J. Phys. Chem. Solids 29, 1337 (1968).
[14]G. Ahlers, Phys. Rev. A 2, 1505 (1970).
[15]J. F. Jarvis, D. Ramm, and H. Meyer, Phys. Rev. 170, 320 (1968).
[16]H. H. Sample and C. A. Swenson, Phys. Rev. 158, 188 (1967).
[17]D. S. Greywall (private communication).
[18]L. H. Nosanow, Phys. Rev. 146, 120 (1966).
[19]N. R. Werthamer, Phys. Rev. A 7, 254 (1972).
[20]H. R. Glyde and F. C. Khanna, Can. J. Phys. 49, 2997 (1971).
[21]H. Horner, J. Low Temp. Phys. 8, 511 (1972).
[22]H. R. Glyde (private communication).
[23]V. V. Goldman, G. K. Horton, and M. L. Klein, Phys. Rev. Lett. 24, 1424 (1970).
[24]T. J. Greytak and J. Yan, Phys. Rev. Lett. 22, 987 (1969).
[25]As pointed out in Ref. 9, a study of the scattered intensity as a function of the incident and scattered polarizations can uniquely identify the c-axis orientation.
[26]N. R. Werthamer (private communication).
[27]W. M. Hartmann and R. J. Elliott, Proc. R. Soc. Lond. 91, 187 (1967).
[28]C. Kittel, *Introduction to Solid State Physics* (Wiley, New York, 1967), 3rd ed., p. 55.
[29]R. J. Birgeneau, L. R. Walker, H. J. Guggenheim, J. Als-Nielson, and G. Shirane, J. Phys. C 8, L328 (1975).
[30]C. M. Varma, Phys. Rev. A 4, 313 (1971).
[31]R. D. Nelson and W. M. Hartmann, Phys. Rev. Lett. 28, 1261 (1972).